

Detection and Characterization of Hepatocellular Carcinoma with Ferucarbotran-Enhanced Perfusion MR Imaging

N. Ogasawara¹, H. Kobayashi¹, K. Shimada¹, Y. Kigami¹, K. Akuta¹

¹Radiology, Otsu Red Cross Hospital, Nagara, Shiga, Japan

Introduction: Feasibility of SPIO-enhanced liver imaging is established for the detection of small liver metastasis. But as for HCC, the efficacy of the study is still unclear because of the lower detectability in cirrhotic patients or the problem of the SPIO-uptake to some well-differentiated HCC. At present, ferucarbotran (Resovist; Schering Japan, Osaka), a new SPIO agent, which allows a rapid bolus injection, is in clinical use. Dynamic study with this agent is expected to assess the tumor vascularity and provide the useful information about differential diagnosis. In this study, we evaluate the ferucarbotran-enhanced perfusion MR imagings using a single-shot echo-planar imaging with SENSE technique, which reduces the susceptibility artifact in EPI sequence, about the detection and characterization of HCC.

Materials and Methods: 34 lesions in 20 patients, diagnosed clinically or histopathologically as HCC, were examined. All the MR studies were performed by 1.5T MR system (Philips Gyroscan Intera Master) with SENSE body coil. Before, during and after 8 micro-mol/kg ferucarbotran administration, in-phase and out-of-phase T1WI, FSE T2WI, GRE T2* and dynamic EPI were obtained. Delayed image of GRE T2* was scanned 10 minutes after SPIO administration. 5 seconds after a bolus injection of SPIO followed by a 20-ml saline flush at the rate of 3 ml/sec, two series of 30 sequential dynamic EPI were obtained under the condition of 30-sec breath holding. About 10 seconds interval for breathing was set between the series. Dynamic study was performed using a single-shot GRE-EPI with SPIR and SENSE techniques. The sequence parameters was as follows: TE/FA = 17ms/20, SENSE factor = 2, acquisition time = 1 sec, Partition = 20, FOV = 280 x 350 mm, Matrix = 102 x 128 / 204 x 256. From the dynamic studies, we evaluated retrospectively the tumor detectability, arrival time of the SPIO to the liver parenchyma and portal vein (PV), early enhancement and washout of the tumor. To hypervascular lesions, functional maps (negative integral maps) during HA phase and PV phase, and serial enhancement ratio images were obtained. From the ROI set to the liver parenchyma and whole of the tumor, time-to-deltaR2* curves were obtained. By the curve analysis, arrival time to the plateau (PT), tumor slope at HA phase (TS) and the mean deltaR2* at HA phase were calculated.

Results: 80% (8/10) of the lesions smaller than 1cm, 89% (8/9) between 1 and 2cm and all lesions (11/11) above 2cm were detected as the signal decrease by the dynamic EPI (Fig1). In all the lesions detectable by dynamic EPI, early enhancement was recognized, but washout within the first dynamic series was unclear in 24% (8/34). All the parameters of PT, TS and the mean deltaR2* during HA phase were significantly different with the liver parenchyma. In 85% (29/34) of the lesions, PTs were earlier than the arrival time to the PV.

Discussion: Ferucarbotran-enhanced dynamic EPI is a promising technique about the detection of hypervascular HCC. 2 of 3 lesions not detected by dynamic EPI were hypovascular tumor, proved by contrast-enhanced dynamic US or CTA. The results suggest this technique could assess the tumor vascularity properly. As has been already reported, prominent characteristics of hypervascular HCC was early enhancement. But in some lesions, washout was not identified. This may be related to SPIO-uptake to the HCC. Earlier PT than arrival time to PV was additional character of hypervascular HCC in this technique. Rapid injection time of no more than 0.5 sec makes it possible. In conclusion, ferucarbotran-enhanced perfusion MR imaging has the excellent detectability of hypervascular HCC and can adequately assess the tumor vascularity.

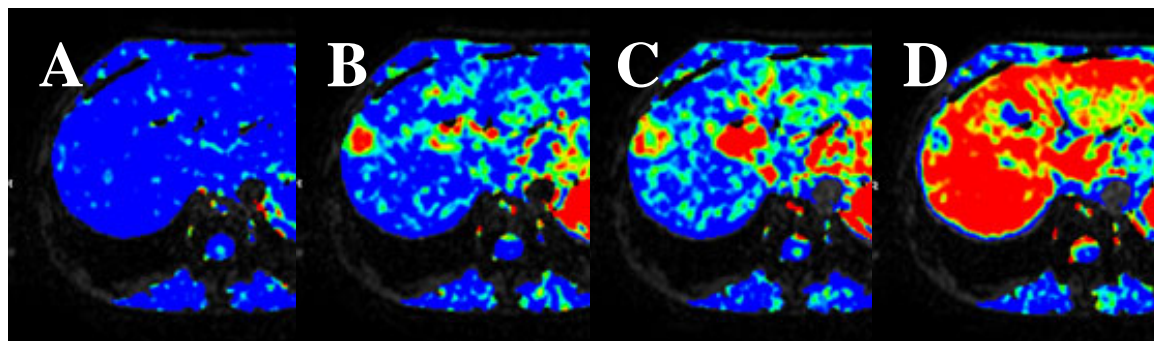


Fig1 HCC in a 62-year-old man. Serial enhancement ratio maps demonstrated hypervascular HCC at early HA phase(B), central washout and coronal enhancement at late HA phase (C) and delayed washout at the second dynamic series (D).